Electronic Supplementary Material (ESI) for Journal of Materials Chemistry A.

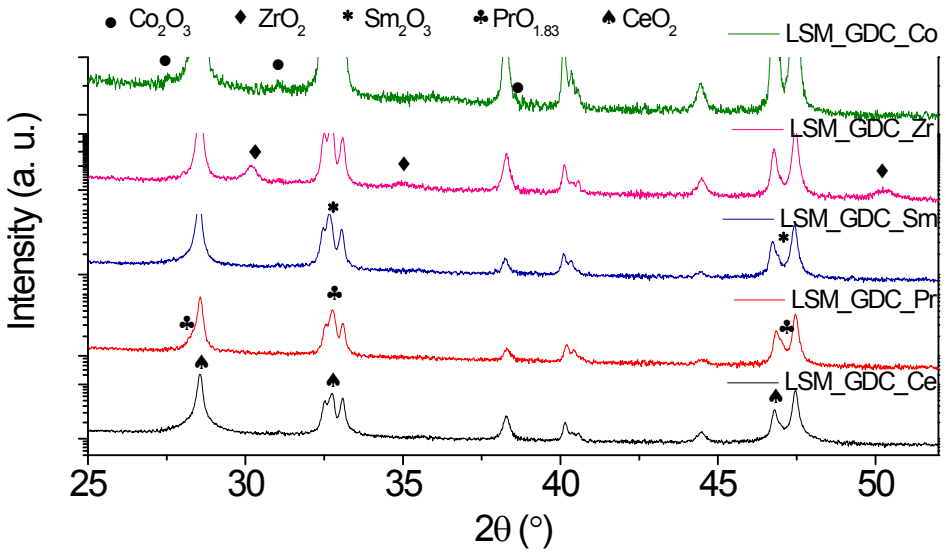

Figure S1: Oxide identification by XRD analysis

XRD patterns of the infiltrated and tested electrodes are showed in the Figure S1. This analysis makes it possible to discern the different oxides infiltrated in the LSM-GDC backbones. Peaks that are not assigned correspond to the LSM and GDC backbone phases.

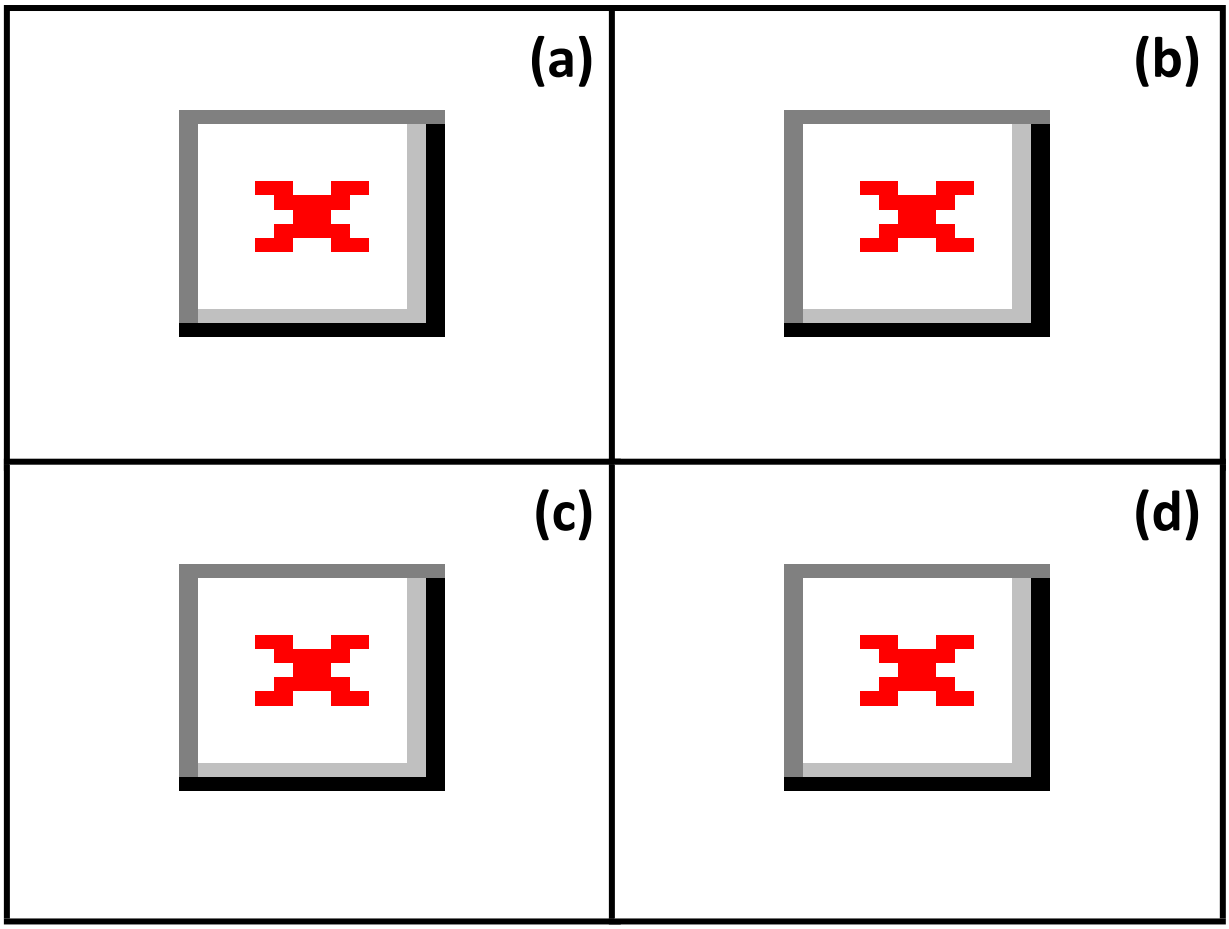

Figure S2: LSM_GDC infiltrated by Pr, calcined at 700 ºC 2h (a) 100K X (c) 10 K X, LSM_GDC infiltrated by Pr, after measurements (b) 100K X (d) 10 K X.

Fracture cross-section SEM images (a) and (c) have been performed from a LSM-GDC backbone infiltrated with Pr and calcined at 700 ºC for 2h, in order to obtain the morphology at the beginning of the EIS measurements. As to discern if there is a change in the morphology of the Pr particles with time, SEM images (b) and (d) were performed after EIS measurements and stability of the symmetrical cell.

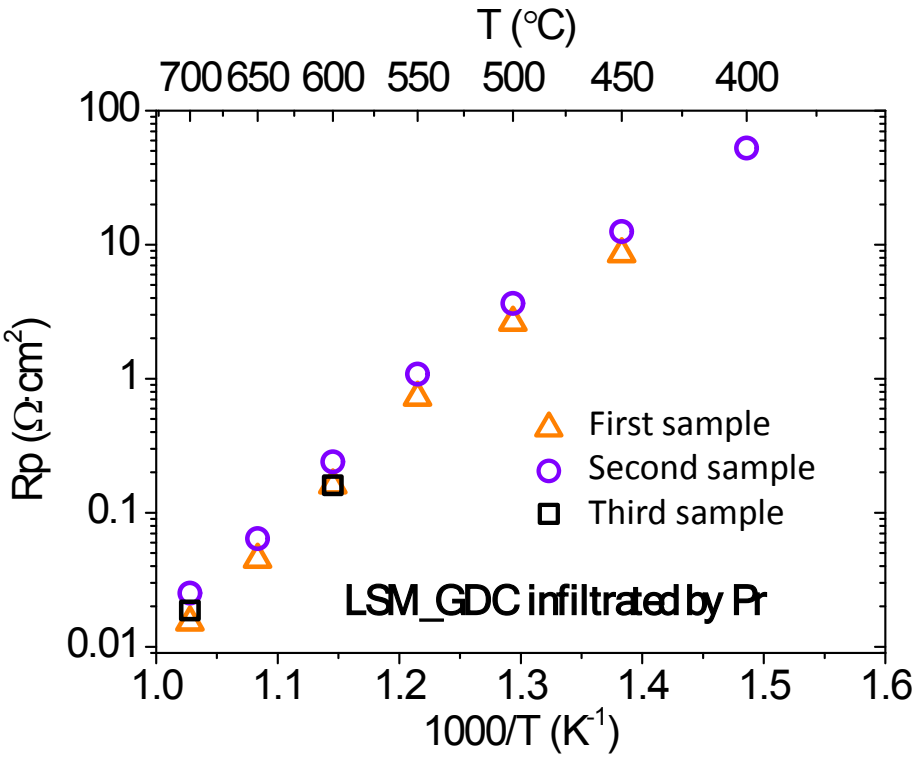

Figure S3: Reproducibility of electrode by means of Polarization resistance on LSM_GDC infiltrated by Pr.

Three different samples infiltrated with Pr precursor were tested by means of EIS measurements in order to check the samples reproducibility.

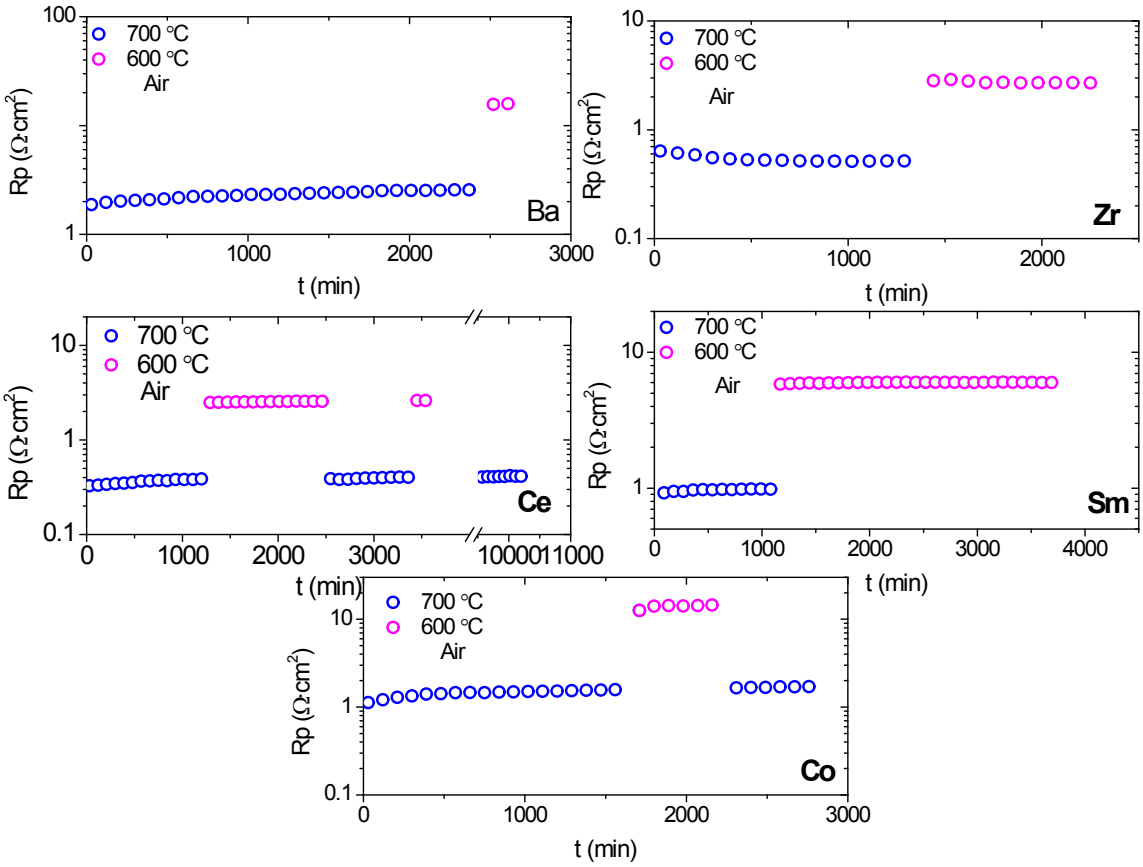

Figure S4: EIS stability of the different LSM-GDC infiltrated backbones.

All symmetrical cells were tested along time at two different temperatures. The element that appears in each plot is the infiltrated oxide.

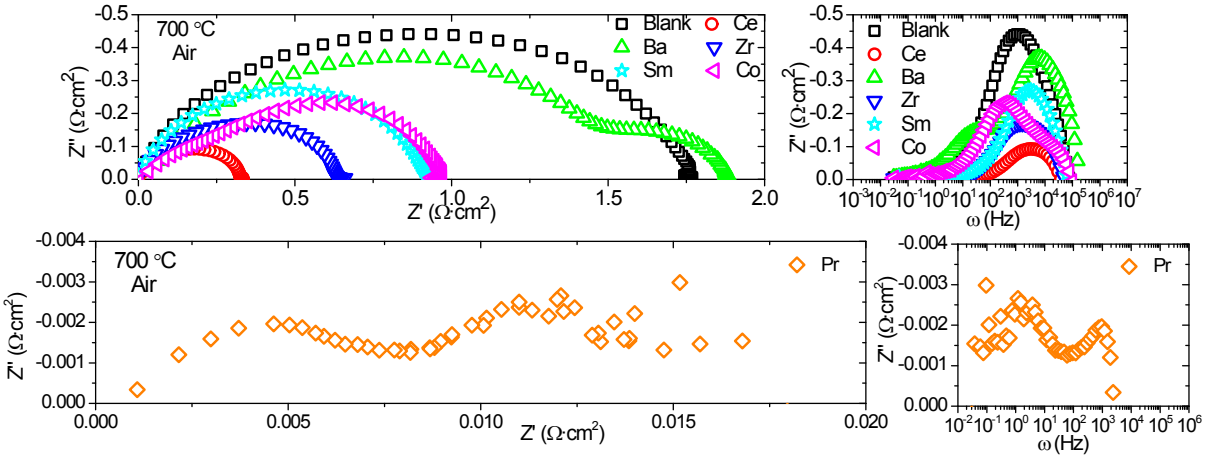

Figure S5: Nyquist and Bode plot of the EIS measurements for the infiltrated and pristine samples at 700 ºC in air.

Results of the figure S5 were obtained for the symmetrical cells. As can be ascribed from the Bode and Nyquist plot, the introduction of the different oxides by means of infiltration reduces the polarization resistance and the limiting resistances are shifted to high frequencies. The ohmic resistances have been subtracted in order to compare only the polarization resistance.

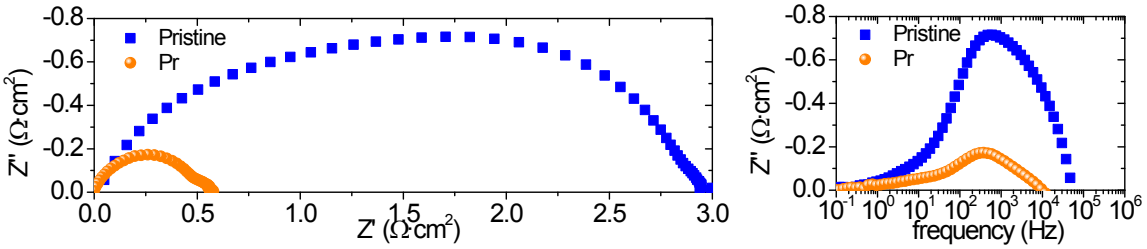

Figure S6: Nyquist and Bode plot of the EIS measurements near the OCV for the fully assembled fuel cell in the fuel cell operation mode at 700 ºC.

The anode-supported fuel cells were based on Ni-YSZ anode and 8 µm-thick YSZ electrolyte. In the fuel cell mode the oxidant feed was air and the fuel wet hydrogen. The cathode was the LSM-GDC backbone and one sample was infiltrated with Pr. The ohmic resistance was subtracted in the Nyquist plot in order to compare the Rp. As can be ascribed from the figure, the resistance at LF and MF were diminished.

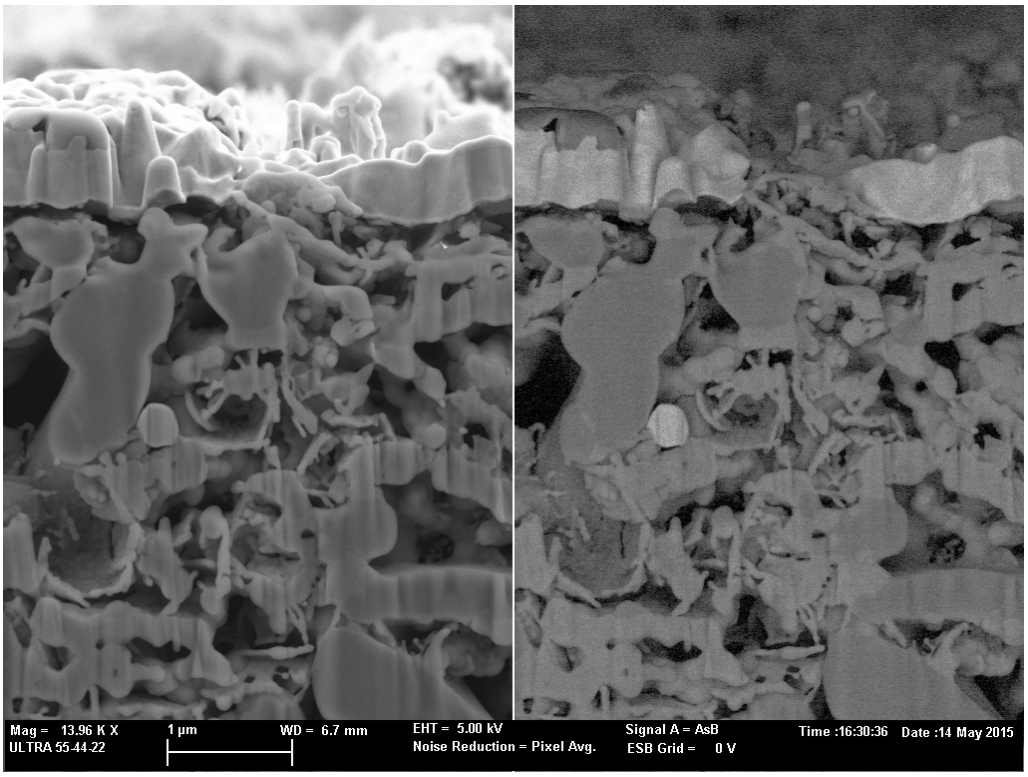

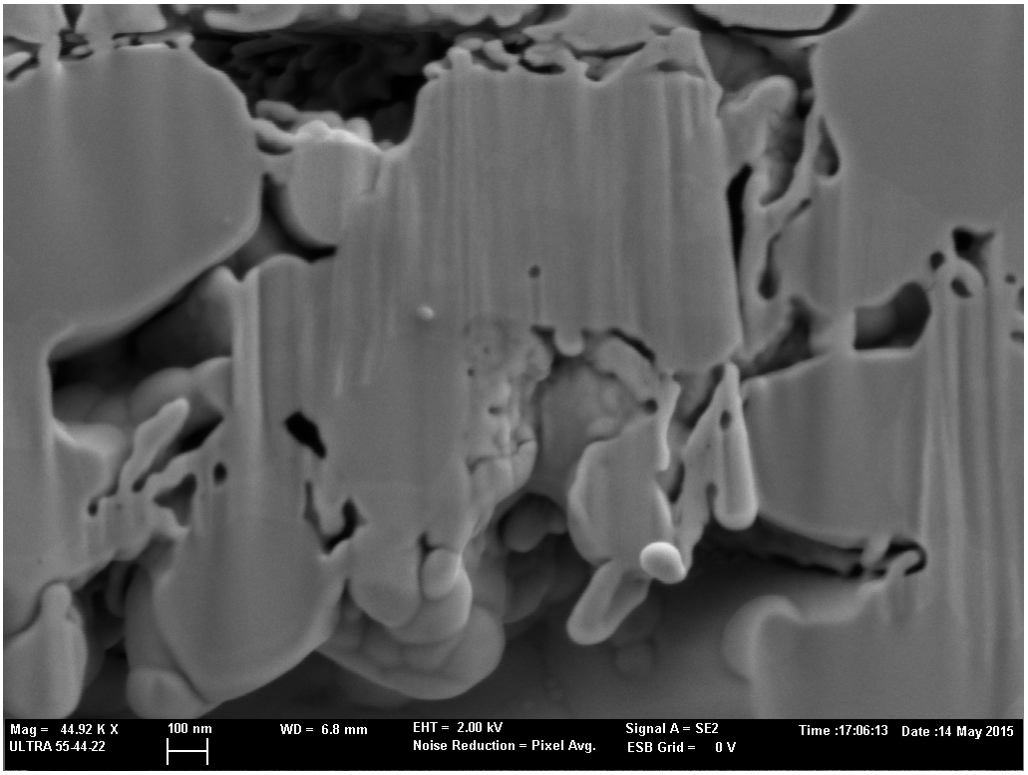

Figure S7: SEM analysis of a FIB-sliced cross-section of the LSM-GDC backbone infiltrated with Pr after electrochemical testing. The top figure are SE (left) and BSE(right) images of the upper side of the electrode and the down figure shows a higher magnification image of electrode particles.

The top images show the top mesh current collector made of gold and illustrates the pore morphology thanks to the FIB preparation method. The higher magnification image (down) shows the PrO_x coating the backbone particles.

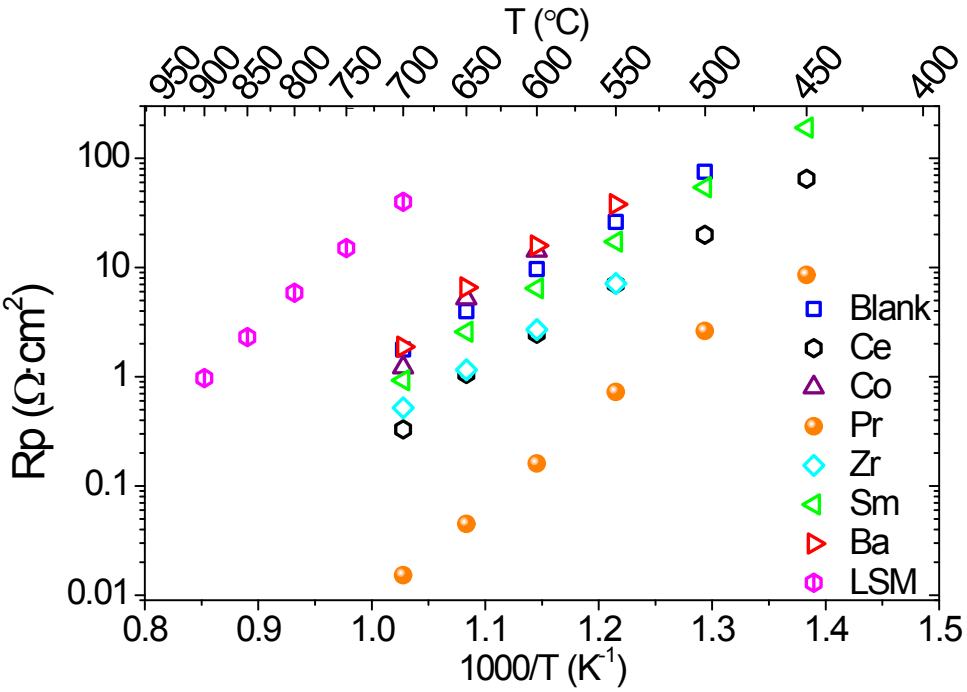

Figure S8: Polarization resistance results for the different promoted cathodes, the pristine electrode and the pure LSM cathode. Results were obtained by means of EIS measurements in symmetrical cells.

Pure LSM cathode exhibits a much higher polarization resistance (more than one order of magnitude) than LSM-GDC composite (blank) and the infiltrated electrodes.